



Since January 2020 Elsevier has created a COVID-19 resource centre with free information in English and Mandarin on the novel coronavirus COVID-19. The COVID-19 resource centre is hosted on Elsevier Connect, the company's public news and information website.

Elsevier hereby grants permission to make all its COVID-19-related research that is available on the COVID-19 resource centre - including this research content - immediately available in PubMed Central and other publicly funded repositories, such as the WHO COVID database with rights for unrestricted research re-use and analyses in any form or by any means with acknowledgement of the original source. These permissions are granted for free by Elsevier for as long as the COVID-19 resource centre remains active.



Review article

Bioactive pyrrole-based compounds with target selectivity

Giovanna Li Petri ^a, Virginia Spanò ^a, Roberto Spatola ^a, Ralph Holl ^b,
 Maria Valeria Raimondi ^{a,*}, Paola Barraja ^a, Alessandra Montalbano ^a

^a Department of Biological, Chemical and Pharmaceutical Sciences and Technologies (STEBICEF), University of Palermo, Via Archirafi 32, 90123, Palermo, Italy

^b Department of Chemistry, Institute of Organic Chemistry, University of Hamburg, Martin-Luther-King-Platz 6, 20146, Hamburg, Germany

ARTICLE INFO

Article history:

Received 21 July 2020

Received in revised form

19 August 2020

Accepted 21 August 2020

Available online 29 August 2020

Keywords:

Pyrrole

Anticancer

Antiviral

Antimicrobial

COVID-19

Targeted compounds

ABSTRACT

The discovery of novel synthetic compounds with drug-like properties is an ongoing challenge in medicinal chemistry. Natural products have inspired the synthesis of compounds for pharmaceutical application, most of which are based on *N*-heterocyclic motifs. Among these, the pyrrole ring is one of the most explored heterocycles in drug discovery programs for several therapeutic areas, confirmed by the high number of pyrrole-based drugs reaching the market. In the present review, we focused on pyrrole and its hetero-fused derivatives with anticancer, antimicrobial, and antiviral activities, reported in the literature between 2015 and 2019, for which a specific target was identified, being responsible for their biological activity. It emerges that the powerful pharmaceutical and pharmacological features provided by the pyrrole nucleus as pharmacophore unit of many drugs are still recognized by medicinal chemists.

© 2020 Elsevier Masson SAS. All rights reserved.

Contents

1. Introduction	2
2. Anticancer activity	2
2.1. Modulators of Bcl-2 family members	2
2.2. Microtubule polymerization-targeting agents (MTs)	2
2.3. Receptor tyrosine kinase (RTKs) inhibitors	3
2.4. CYP1 inhibitors	7
2.5. Inhibitors of NF- κ B and ICB2 interaction	7
2.6. Hypoxia-inducible factors (HIFs) inhibitors	7
3. Antimicrobial activity	7
3.1. Sortase A (SrtA) inhibitors	7
3.1.1. 2-Trans-enoyl-acyl carrier protein reductase (InhA) inhibitors	8
4. Antiviral agents	8
4.1. HIV-1 integrase (IN) inhibitors	8
4.2. Non-nucleoside HCV non-structural protein 5B (NS5B) polymerase inhibitors	9
4.3. RNA-dependent RNA polymerase (RdRp) inhibitors for Ebola virus disease	9
5. Concluding remarks	10
Funding source	10
Declaration of competing interest	10
Abbreviations	10
Supplementary data	11
References	11

* Corresponding author.

E-mail address: mariavaleria.raimondi@unipa.it (M.V. Raimondi).

1. Introduction

For thousands of years, natural products from plants, animals or microbes have been used to treat pathological conditions [1]. The development of compounds with desired physicochemical properties, pharmacokinetic, and pharmacodynamic profiles is an essential issue of medicinal chemistry, which can benefit from the support of *in silico* studies [2–4]. Incessant optimization of lead compounds to obtain new drug-like molecules represents the pivotal challenge of drug discovery [5–8]. The use of heterocycles as bioisosteres for a variety of functional groups is a strategic path to obtain clinically safer drugs, thereby increasing affinity and potency towards their respective targets [9,10]. Furthermore, heterocyclic moieties can modulate properties such as solubility, lipophilicity, polarity, and hydrogen bonding capacity [2,11].

According to an analysis conducted by Vitaku et al. on U.S. FDA-approved small-molecules, *N*-heterocycles are the most common structural skeletons of pharmaceuticals on the market. Indeed, approximately 84% of the total number of molecules contain at least one nitrogen atom, while 59% contain at least one nitrogen heterocycle [12]. Additionally, in a recent analysis reported by Martins and collaborators [13] on oncological drugs approved by the FDA between 2010 and 2015, the use of heterocycles in drug discovery was further emphasized. In that time frame, 26 out of 40 newly approved chemotherapeutic drugs contained heterocyclic fragments in their molecular composition. Among these heterocycles, 73% were nitrogen-based, surpassing by far the number of nitrogen-oxygen- (15%), oxygen- (8%), and nitrogen-sulfur-based (4%) heterocycles.

In Table 1, some of the most representative clinically used pyrrole-based drugs approved by the FDA are summarized. Among these, the antiviral agent remdesivir, which is nowadays in clinical trials as promising drug for the treatment of patients affected by COVID-19, a virus strain first identified in Wuhan, Hubei Province, China, spreading among humans since December 2019 [14]. Wu et al. performed docking studies with the aim of evaluating potential targets of remdesivir [15]. The results showed a *mfScores* of –112.8 for RdRp, highlighting the role of the pyrrolotriazine moiety of remdesivir, which generates hydrophobic interactions with Tyr131 and Tyr401. Therefore, remdesivir represents a promising lead to develop other analogs to counteract *coronavirus* infections.

In this review, we analyzed the most representative targets of recently developed pyrrole-based compounds, including also hetero-fused derivatives, within selected therapeutic areas such as anticancer, antimicrobial and antiviral. In particular, we explored the literature between 2015 and 2019, selecting the most relevant papers, in which a specific target was identified in the biological response and in which structure-activity relationships (SAR) were analyzed to elucidate the selectivity toward the target assessed in the study. Indole derivatives were not included because the topic is so extensive that it deserves a dedicated discussion.

2. Anticancer activity

Cancer is one of the biggest health problems worldwide, representing the second leading cause of death in the United States (US). Siegel et al. estimate 1,806,590 new cancer cases and 606,520 cancer deaths in the US in 2020 [16]. Despite the increasing numbers compared to the 2019 estimation [17], cancer deaths are supposed to decline, indicating that cancer therapy is improving year after year. Certainly, molecular targeted therapy contributes to the improvement of this general trend [18–20]. Table 2 shows the main anticancer targets addressed by pyrrole-based compounds.

2.1. Modulators of Bcl-2 family members

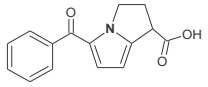
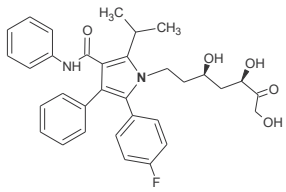
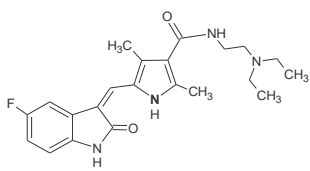
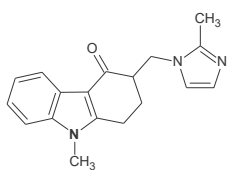
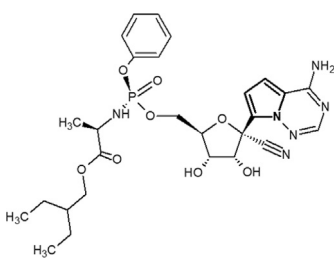
Several pyrrole derivatives exhibit antitumor activity by triggering apoptosis events, a highly regulated and controlled process inducing programmed cell death. This process can occur via the extrinsic or intrinsic signalling pathways, which both lead to the activation of proteases, namely caspases. While the first pathway is activated via death receptors, the intrinsic one is activated by internal stimuli that cause mitochondrial oxidative stress [21]. In 2019, Kilic-Kurt et al. [22] reported pyrrolo[2,3-*d*]pyrimidines bearing an urea moiety at position 2 of the scaffold, which exhibit cytotoxic activity against A549, PC-3, and MCF-7 cell lines. Cytotoxicity was influenced by the decoration of the scaffold. A549 cells were particularly sensitive to the treatment with compounds **1a,c,d**, showing IC_{50} s of 0.35, 1.48, and 1.56 μ M, respectively. In contrast, compound **1b** was more active against PC-3 cells ($IC_{50} = 1.04 \mu$ M). Additionally, the results of an annexin V binding assay and Western blot analysis showed that the most promising compounds **1a,c,d** induced apoptosis in A549 and HCT116 wt cells through the intrinsic apoptotic pathway by activating the proapoptotic proteins Bim, Bax, Bak, and Puma, and by deactivating anti-apoptotic proteins, including Bcl-2, Mcl-1, and Bcl-XL, thereby inducing the activation of caspase-3, caspase-9 and the cleavage of poly(ADP-ribose)polymerase (PARP) enzymes.

2.2. Microtubule polymerization-targeting agents (MTs)

Microtubules (MTs) represent an important target in the area of anticancer therapy. They are the main constituent of the cell cytoskeleton involved in the mitosis phases of mammalian cells. MTs consist of $\alpha\beta$ -tubulin heterodimers that polymerize by a non-covalent nucleation-elongation mechanism. Modification of MT dynamics can lead to cell cycle arrest and in consequence to cell death by apoptosis in dividing cells [23].

In 2017, Carta et al. [24] investigated the antiproliferative activity of novel phenylpyrroloquinolinones (PPyQs) against a panel of leukemic and solid tumor cell lines. The best effect was achieved by compound **2**, bearing a benzoyl group at the pyrrole nitrogen, instead of a sulfonyl or carbamoyl moiety, reaching GI_{50} s of 0.2, 0.1, and 0.2 nM against HeLa, HT-29, and MCF-7 cell lines, respectively. The cytotoxic potential of **2** was assayed *in vitro* against peripheral blood lymphocytes from healthy donors. Its effects in quiescent lymphocytes ($GI_{50} = 28 \mu$ M) and in phytohemagglutinin-stimulated lymphocytes ($GI_{50} = 15 \mu$ M) revealed its selectivity for quickly proliferating cells. Moreover, compound **2** caused a G2/M arrest in a concentration dependent manner, both in HeLa and Jurkat cell lines, strong inhibition of tubulin assembly with an IC_{50} of 0.89 μ M (combretastatin A-4, CA-4 $IC_{50} = 1.2 \mu$ M), and 70% inhibition of colchicine binding at 5 μ M (CA-4 = 98% at 5 μ M). Docking studies (PDB ID: 5C8Y) indicated a similar binding mode of **2** as for the known inhibitor plinabulin, as showed in Fig. 1. The same group of authors [25] further investigated the role of the angular geometry and of the substituents at positions 3 and 7. The presence of a naphthalene or benzodioxole moiety at position 7 and [3,2-*g*] and [3,2-*h*] geometries led to enhanced cytotoxicity. [3,2-*f*]-PPyQ **3**, bearing a 7-benzodioxole moiety and a 3-ethyl group, was identified as a powerful selective inducer of apoptosis in the A549 and HeLa cell lines. The antiapoptotic activity was mainly attributed to the generation of reactive oxygen species (ROS) and the decreased expression of anti-apoptotic proteins, such as Bcl-2 and Mcl-1. Compound **3** was as potent as **2** in inhibiting tubulin assembly (IC_{50} of 0.84 μ M), but less effective in inhibiting colchicine binding (49%). Although exhibiting the same binding mode as **2**, docking studies revealed that compound **3** is able to establish an additional H-bond with β -tubulin through its benzodioxole group.

Table 1
Representative pyrrole-based drugs on the market.

Pharmacological Application	Drug	Chemical structure	Target
Anti-inflammatory	Ketorolac (Lemmon Company)		Cyclooxygenases (COXs)
Anti-lipidemic	Atorvastatin (Pfizer Ireland Pharmaceuticals)		HMG CoA reductase
Antitumor	Sunitinib (Pfizer, Inc.)		Platelet-derived growth factor (PDGF-Rs) and vascular endothelial growth factor receptors (VEGFRs)
Antiemetic	Ondansetron (Glaxo Wellcome Inc)		Serotonin receptors of the 5-HT3 type
Antiviral	Remdesivir (Gilead Sciences Inc)		viral RNA-dependent RNA polymerase (RdRP)

Fluorinated 7-PPyQ analogs **4–6** [26] retained high cytotoxicity with GI_{50} values at the nanomolar level and strong cytotoxicity also in the multidrug-resistant CEM^{Vbl100} cell line with GI_{50s} of 0.8–44 nM, proposing that their mechanism of action does not involve P-glycoprotein. The N-ethyl derivative **4**, bearing a 2-fluorine substituted aryl moiety at position 7, caused G2/M phase arrest, apoptosis with ROS production, activation of caspase-3 and PARP, and a decrease in the expression of anti-apoptotic proteins. A stronger inhibition of tubulin assembly ($IC_{50} = 0.38 \mu M$) and colchicine binding (70%) was observed, but the presence of fluorine did not significantly affect the binding mode as confirmed by docking studies. Finally, *in vivo* studies showed that compounds **4** and **6** decreased tumor mass in a murine model at doses four times lower than CA-4.

In 2019, Brindisi et al. [27] synthesized a new series of pyrrolonaphthoxazepines and evaluated their effects on cell cycle, apoptosis, and differentiation in a variety of cancer cells. Among all, compound **7** showed the best antiproliferative activity against HL-60 cells with an IC_{50} of 294.5 nM, causing G2/M arrest at 10 μM . Compound **7**, containing a 5-quinoline moiety, showed the best activity in inhibiting tubulin polymerization, monitored by turbidity experiments, at sub-stoichiometric concentrations in a colchicine-like manner, suggesting that it may inhibit tubulin assembly by binding to the colchicine site (PDB ID: 4O2B and 1JFF).

2.3. Receptor tyrosine kinase (RTKs) inhibitors

Tyrosine kinase proteins have been identified as a large multi-gene family, whose activation/inactivation is crucial for numerous signalling pathways that mediate cell-to-cell communication. Due to their roles as growth factor receptors, their inhibition can interfere with cancer progression [28,29]. According to the Human Genome Project, 90 genes code for tyrosine kinases, among which 58 are receptor-type tyrosine kinases, being subdivided into 20 subfamilies, and 32 are non-receptor tyrosine kinases, being divided into 10 subfamilies. Among these receptors, the epidermal growth factor receptor (EGFR), the platelet-derived growth factor receptors (PDGFR), the fibroblast growth factor receptor (FGFR), the vascular endothelial growth factor (VEGF) receptor, the angiotensin (Tie) receptor, Met (hepatocyte growth factor/scatter factor (HGF/SF) receptor), the ephrin (Eph) receptor, the tropomyosin kinase (Trk) receptor, and the insulin receptor are the most abundant RTKs. Simultaneous inhibition of multiple kinases has been proposed to afford synergistic effects compared to the silencing of only one type, as well as to circumvent drug resistance.

In 2018, Kurup et al. [30] reported the synthesis of eighteen pyrrolo [2,3-*d*]pyrimidines as dual inhibitors of aurora kinase A (AURKA) and EGFR, which are involved in the regulation of important processes including cell proliferation, survival, differentiation, and migration.

Table 2
Anticancer activity of pyrrole derivatives 1–21.

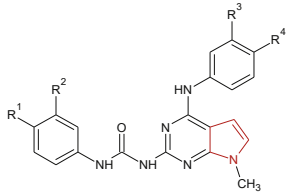
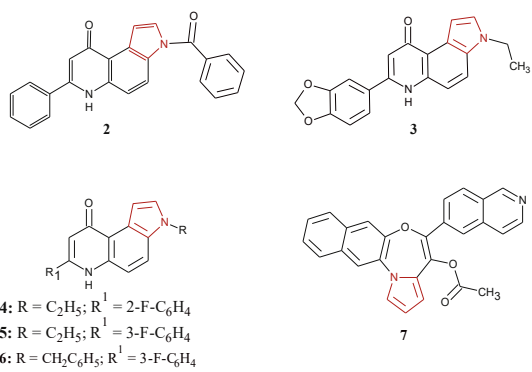
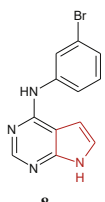
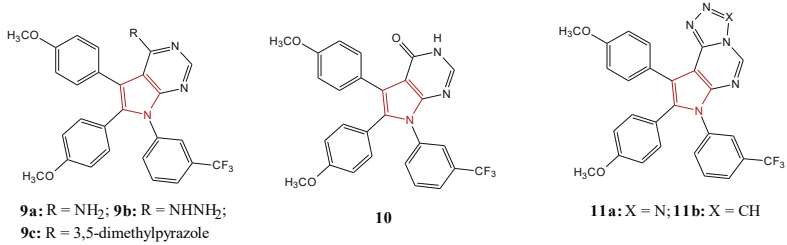
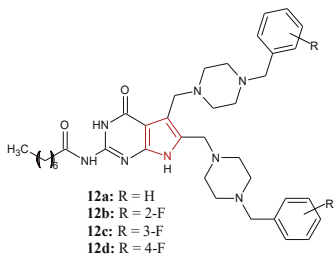
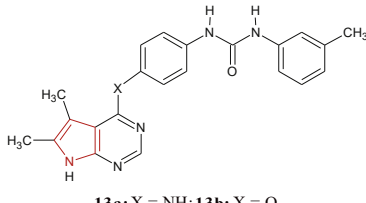
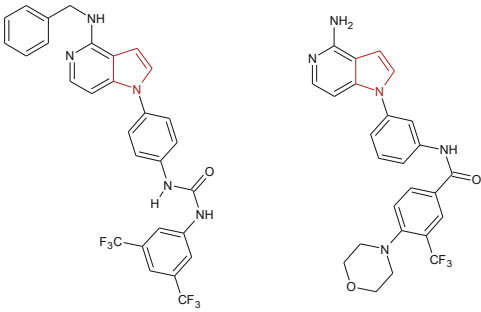
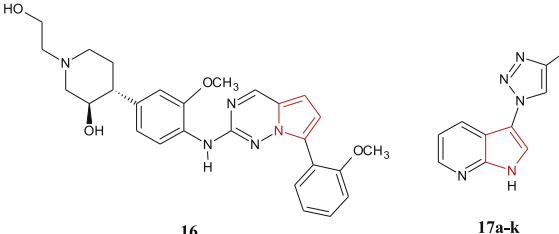
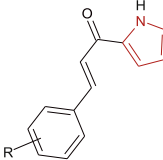
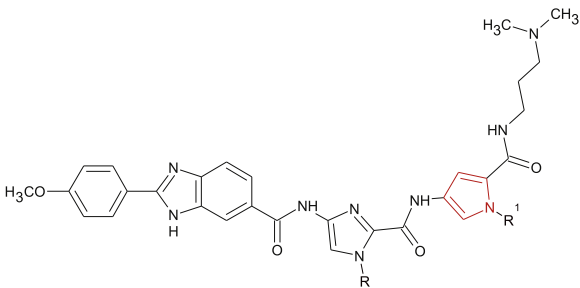
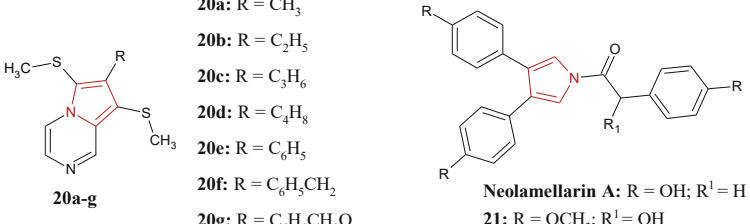
Targets	Chemical structures
Activation of: Bim, Bax, Bak, Puma Deactivation of: Bcl-2, Mcl-1 and Bcl-XL	 <p>1a-d</p> <p>1a: R¹ = H; R² = CF₃; R³ = Cl; R⁴ = F 1b: R¹ = Cl; R² = CF₃; R³ = Br; R⁴ = H 1c: R¹ = F; R² = CF₃; R³ = Br; R⁴ = H 1d: R¹ = F; R² = R³ = H; R⁴ = Cl</p>
Microtubules (MTs)	 <p>4: R = C₂H₅; R¹ = 2-F-C₆H₄ 5: R = C₂H₅; R¹ = 3-F-C₆H₄ 6: R = CH₂C₆H₅; R¹ = 3-F-C₆H₄</p> <p>7</p>
EGFR and AURKA kinases	 <p>8</p>
PKCa, JNK2, TrkA, ERK1, MAPKAP-K3, CAMK1, MINK1 and VEGFR kinases	 <p>9a: R = NH₂; 9b: R = NHNH₂; 9c: R = 3,5-dimethylpyrazole</p> <p>10</p> <p>11a: X = N; 11b: X = CH</p>
FGFR4, Tie2 and TrkA kinases	 <p>12a: R = H 12b: R = 2-F 12c: R = 3-F 12d: R = 4-F</p>
VEGFR-2 kinase	 <p>13a: X = NH; 13b: X = O</p>

Table 2 (continued)

Targets	Chemical structures
FMS kinase	 <p>14</p> <p>15</p>
ALK kinase	 <p>16</p> <p>17a-k</p> <p>17a: R = C₆H₅ 17b: R = C₆H₄-4-CH₃ 17c: R = C₆H₄-4-C(CH₃)₃ 17d: R = (CH₂)₃CH₃ 17e: R = cyclopropyl 17f: R = C(CH₃)₂OH 17g: R = CH₂(CH₂)₂OH 17h: R = OC(O)CH₂CH₃ 17i: R = CH₂OH 17j: R = C₆H₄-4-F 17k: R = C₆H₄-4-OCH₃</p>
CYP1 inhibitors	 <p>18a: R = 2-OCH₃; 18b: R = 2-Cl</p>
Nuclear Factor Y (NF-Y)	 <p>HxIP: R = CH₃; R¹ = CH₃; 19a: R = CH₃; R¹ = (CH₂)₃NH₂; 19b: R = (CH₂)₃NH₂; R¹ = CH₃</p>
Hypoxia-inducible factors (HIFs)	 <p>20a: R = CH₃ 20b: R = C₂H₅ 20c: R = C₃H₆ 20d: R = C₄H₈ 20e: R = C₆H₅ 20f: R = C₆H₅CH₂ 20g: R = C₆H₅CH₂O</p> <p>Neolamellarin A: R = OH; R¹ = H 21: R = OCH₃; R¹ = OH</p>

Enzymatic assays were conducted to evaluate the ability of all compounds to inhibit the kinases and the results showed nanomolar and micromolar inhibition of EGFR and AURKA, respectively. The best dual activity was exhibited by compound **8**, which showed IC₅₀s of 1.99 μM against AURKA and 3.76 nM against EGFR. A SAR

analysis revealed that the presence of halogens on the 4-anilino moiety was pivotal for dual EGFR and AURKA inhibition. Finally, docking studies were performed to evaluate the interactions within the ATP pockets of EGFR (PDB ID: 3W33) and AURKA (PDB ID: 4BYI). Binding results on EGFR revealed a H-bond between the free NH

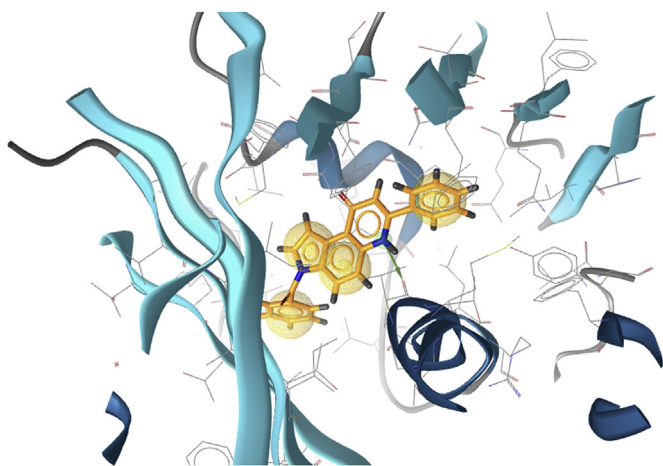


Fig. 1. Observed binding mode of compound **2** (orange stick) docked into the crystal structure of T2R-TTL-Plinabulin complex (B) (PDB ID: 5C8Y) and examined by LigandScout® version 4.4 Expert (Inte:Ligand, GmbH). Green arrow represents donor hydrogen bond; yellow spheres represent hydrophobic interactions. (For interpretation of the references to color in this figure legend, the reader is referred to the Web version of this article.)

pyrrole and the backbone carbonyl of Met793 as crucial contact. Similar docking results were obtained when docking compound **8** into the ATP pocket of AURKA.

In 2015, Ibrahim et al. [31] synthesized pyrrolopyrimidines **9a-c**, pyrrolopyrimidone **10**, pyrrolotetrazolopyridine **11a**, and pyrrolotriazolopyridine **11b**, which demonstrated interesting anti-proliferative activities against the A375 cell line, with IC_{50} s ranging from 8.55 to 23.45 μ M. Inhibitory activities against a panel of 124 kinases were also determined. The results showed that all compounds exhibited kinase selectivity for PKCa, JNK2, TrkA, ERK1, MAPKAP-K3, CAMK1, MINK1, and VEGFR, inhibiting their activity by more than 50% at 25 nM. Structural variations of the pyrrolopyrimidine nucleus caused no significant changes in enzyme inhibitory activities. However, among all, the tetrazolyl and triazolyl (**11a,b**) and the 3,5-dimethylpyrazole (**9c**) moieties, directed the antitumor activity against A375.

Recently, Lee et al. [32] synthesized two series of 5-substituted and 5,6-disubstituted pyrrolo[2,3-*d*]pyrimidine octamides and tested their *in vitro* antiproliferative activity against three human cancer cell lines, including MCF-7, SKBR3, and HCT116. All compounds exhibited good antiproliferative activity with micromolar GI_{50} values and selectivity for cancer cells, as demonstrated by low cytotoxic effects ($GI_{50} > 10.0$ μ M) against HFF-1 cells. The *in vitro* kinase screening conducted with the most active compounds **12a-d** revealed their highly selective inhibitory activity towards FGFR4 ($IC_{50} = 6.71$ – 7.67 μ M), Tie2/Tek ($IC_{50} = 5.80$ – 8.69 μ M), and TrkA ($IC_{50} = 2.25$ – 3.15 μ M). The presence and the position of fluorine substituents did not significantly affect kinase selectivity.

Angiogenesis is an important process for tumor growth due to the development of new blood vessels that allow the supply of oxygen and nutrients to the proliferating cells, thereby causing cancer progression and metastasis [33]. The VEGF family, which includes VEGF-A, VEGF-B, VEGF-C, VEGF-D, and placental growth factor (PlGF), represents a group of key proteins involved in the angiogenic pathway [34]. VEGF inhibitors bind three different RTKs: VEGFR-1, VEGFR-2, and VEGFR-3, which are expressed on the lymphatic and vascular endothelium. VEGFR-2 is the main mediator of the VEGF-induced angiogenic signalling and its activation leads to cell proliferation, migration, permeability, and survival, thus resulting in vasculogenesis and angiogenesis [35].

Based on docking studies reported in the literature on the powerful VEGFR-2 inhibitor sorafenib, in 2018, Adel et al. [36] designed and synthesized a series of pyrrolo[2,3-*d*]pyrimidines to test their ability to inhibit VEGFR-2 *in vitro*. All tested compounds showed highly potent dose-related VEGFR-2 inhibition with IC_{50} s in the nanomolar range. Among all, compounds **13a,b** exhibited IC_{50} values of 11.9 and 13.6 nM, respectively. Docking into the active site of VEGFR-2 (PDB ID: 3VHE) was performed, confirming the interactions between the pyrrolo[2,3-*d*]pyrimidines and VEGFR-2.

The Feline McDonough Sarcoma (FMS) kinase is a member of the PDGFR family of class-III RTKs. The binding of the macrophage or monocyte colony-stimulating factor (M-CSF or CSF-1) induces its activation, followed by oligomerization and transphosphorylation processes, and the consequent modulation of the survival, proliferation, and differentiation of monocyte/macrophage lineage. Mutations in the gene coding for the FMS kinase or the over-expression of CSF-1 have been associated with a predisposition to myeloid malignancy, as well as other disease conditions, including osteoclast proliferation in bone osteolysis and inflammatory illnesses [37].

In 2018, El-Gamal and Oh [38] synthesized a series of pyrrolo[3,2-*c*]pyridines to test their inhibitory effect against the FMS kinase. Among all, compounds **14** and **15** were the most potent showing IC_{50} s of 60 and 30 nM, respectively. Their activity was related to the 3,5-bis(trifluoromethyl)phenyl substituent of diarylurea derivative **14** and to the 4-morpholino-3-(trifluoromethyl)phenyl substituent of diarylamide **15**, which enhanced the affinity to the enzyme. Compound **15** was selected for further screenings and its antiproliferative effects were evaluated against thirteen cancer cell lines (ovarian, prostate, and breast) showing IC_{50} s from 0.15 to 1.78 μ M, and selectivity towards cancer cells over normal fibroblasts. A potent effect was also observed against bone marrow-derived macrophages, inhibiting their CSF-1-induced growth with an IC_{50} value of 84 nM. The selectivity of compound **15** was confirmed over a panel of 40 kinases, inhibiting the FMS kinase by 81% at 1 μ M.

The Anaplastic Lymphoma Kinase (ALK) is a transmembrane tyrosine kinase receptor, which, after binding of a specific ligand, undergoes dimerization and successive autophosphorylation of the intracellular kinase domain. ALK gene activation is involved in the carcinogenesis process of several human cancers, such as anaplastic large cell lymphoma, lung cancer, inflammatory myofibroblastic tumors, and neuroblastoma, as a consequence of fusion with other oncogenes (NPM, EML4, TIM, etc.) or gene amplification, mutation or protein overexpression [39].

In 2015, Mesaros et al. [40] carried out the diastereoselective synthesis of pyrrolo [2,1-*f*] [1,2,4]triazine derivatives that exhibited excellent *in vitro* ALK inhibitory activities, both in an enzyme (IC_{50} s of 3–57 nM) and a cell-based assay (IC_{50} s of 30–500 nM). These excellent *in vitro* results prompted the authors to investigate the *in vivo* inhibition of ALK autophosphorylation, which was performed only with *cis* and *trans* piperidine-3-ol-derived pyrrolo-triazines. Among these, the *trans*-4-aryl-piperidine-3-ol **16** was most active, thus indicating a strong influence of the stereochemistry on the biological activity.

In 2016, Narva and co-workers [41] synthesized new pyrrolo [2,3-*b*]pyridines to evaluate their antitumor activity against the three human cancer cell lines A549, HeLa, and MDA-MB-231. Among all, compounds **17a-k** showed their maximum growth inhibitory effect at concentrations from 0.17 to 25.9 μ M). In contrast to compounds with electron-donating substituents including methoxy (**17k**), methyl (**17b**), and *t*-butyl (**17c**) as well as the unsubstituted one (**17a**), compound **17j**, possessing a fluorine-substituted phenyl ring, showed good activity against all three cell lines with GI_{50} values in the range of 0.18–0.7 μ M.

Nevertheless, docking studies indicated that compounds **17f,g,i**, bearing a hydroxy group, should be able to bind to the ALK active site (PDB ID: 2XP2) with an affinity comparable to that of crizotinib.

2.4. CYP1 inhibitors

Cytochrome-P450 (CYP) is a superfamily of enzymes, some of which are responsible for phase-1 metabolism. The CYP1 subfamily includes 1A1, 1B1, and 1A2 isoforms. The CYP1A1 isoform is involved in the hydroxylation of various pro-carcinogens and, when overexpressed, it can convert benzo[a]pyrene [BaP] into benzo[a]pyrene-7,8-dihydrodiol-9,10-epoxide, a quinone derivative which binds and damages DNA. Similarly, the overexpression of CYP1B1 in cancer cells leads to the increased metabolism of cisplatin, resulting in the reduction of its activity and chemoresistance. In 2017, Williams et al. [42] designed and synthesized a series of 2-pyrrole-based chalcones as potential inhibitors of CYP1, CYP2, and CYP3, in order to overcome CYP1A1-mediated BaP toxicity and CYP1B1-mediated cisplatin resistance. All synthesized compounds were inactive against CYP2C9, CYP2C19, and CYP3A4 isoforms and only slightly active against CYP2D6. Moreover, all compounds inhibited at least one CYP1 isoform, with compound **18a** inhibiting all CYP1 isoforms with approximately equal potency (IC₅₀s of 0.9–1.1 μM) and compound **18b** selectively inhibiting CYP1B1 with an IC₅₀ of 0.21 μM. SAR investigations indicated that halogen or methoxy substituents on the phenyl ring were essential for activity. This data were confirmed by testing both **18a,b** in HEK293 cells. It was found that compound **18a** inhibited the 1A1 and 1B1 isoforms with a comparable efficacy (IC₅₀ = 1.2 μM) and was able to rescue cells from BaP toxicity. Instead, compound **18b** was selective only for CYP1B1 (IC₅₀ = 0.25 μM), thus reversing cisplatin resistance. The direct interaction of compounds **18a,b** with CYP1A1 (PDB ID: 4I8V) and CYP1B1 (PDB ID: 3PM0) was confirmed by docking studies.

2.5. Inhibitors of NF- κ B and ICB2 interaction

Nuclear Factor- κ B (NF- κ B) is a transcription factor, which interacts with the ICB2 site in the promoter of topoisomerase-II α (topo-II α) to regulate the expression of the aforesaid enzyme. Topo-II α is crucially involved in DNA metabolism and is targeted by many anticancer drugs, such as etoposide and doxorubicin. The interaction between NF- κ B and ICB2 is linked to the confluence-induced downregulation of topo-II α and the consequential resistance to topo-II α targeting drugs. In 2017, Pett et al. [43] designed and synthesized pyrrole-polyamides, incorporating the *p*-anisylbenzimidazole (Hx) DNA recognition element, to target the 5'-flanking sequence 5'-TACGAT-3' of the ICB2, and disrupt the interaction between NF- κ B and ICB2. Compound **19a** was shown to display a dose-dependent inhibition of NF- κ B binding to the ICB2 at doses ≥ 3 μM using an electrophoretic mobility shift assay (EMSA). Additionally, compound **19a** was found to be able to remove NF- κ B already bound to the ICB2. The capacity of **19a** in mediating the chemosensitisation to the cytotoxic effects of etoposide and doxorubicin was evaluated in confluent A549 cells. The synergistic effect of etoposide (400 μM) combined with **19a** (5 μM) decreased cell viability by an additional 50% in comparison with the treatment with etoposide alone. Moreover, pre-treatment with **19a** at 5 μM increased the sensitivity to doxorubicin, producing an additional 22% reduction in cell viability with respect to the treatment with doxorubicin alone (75 μM). A better DNA binding affinity of **19a** (0.5 μM) with the ICB2 site was demonstrated compared to reference compound **HxIP**, bearing methyl groups on the pyrrole and the imidazole ring (1 μM), and regioisomer **19b**, bearing the propyl-amino group at the imidazole nucleus (3 μM). Differences between

the two polyamides **19a** and **19b** in DNA binding affinities could be due to electrostatic repulsions between the positively charged groups and steric effects between the alkyl chains.

2.6. Hypoxia-inducible factors (HIFs) inhibitors

Hypoxia-inducible factors (HIFs) are transcriptional heterodimer complexes consisting of an inducible α -subunit (HIF-1 α , HIF-2 α , HIF-3 α) and constitutively expressed β -subunits. They are responsible for regulating the response of cancer cells in a hypoxic environment. HIFs is the major regulator of the transcription of genes involved in cancer pathobiology, such as cell proliferation, angiogenesis, metabolism, and invasion. In 2016, Lee and co-workers [44] synthesized a series of pyrrolo[1,2-*a*]pyrazines **20a-g** variously substituted in position 7 with alkyl chains or an additional aromatic group and tested their activity as HIF-1 α inhibitors. Analogs with longer alkyl chains (**20b-d**) showed stronger inhibitory effects on insulin-induced HIF-1 α accumulation, whereas the introduction of a phenyl ring (**20e**) reduced activity. However, aromatic substituents with suitable alkyl linkers, such as benzyl (**20f**) and phenethyl (**20g**) groups, led to enhanced HIF-1 α inhibitory activities (81% and 87% at 10 μM, respectively).

In 2019 [45], the discovery of the HIF-1 inhibitor activity of the marine pyrrole-alkaloid neolamellarin A, derived from sponges, inspired the synthesis of new analogs which were tested for their HIF-1 inhibitory activity and cytotoxicity in HeLa cells. The biological results showed that neolamellarin A and its derivative **21** had the best HIF-1 inhibitory activity with IC₅₀s of 10.8 and 11.9 μM, respectively. Interestingly, compared to the two-carbon aliphatic chain linker neolamellarin A, the introduction of a single or triple aliphatic chain between the pyrrole and phenyl ring reduced the inhibitory activity (IC₅₀s of 18.8 and 14.7 μM, respectively), whereas a *trans*-olefin chain strongly diminished activity (IC₅₀ > 50 μM), probably due to the greater rigidity granted to the structure.

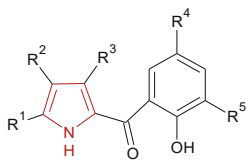
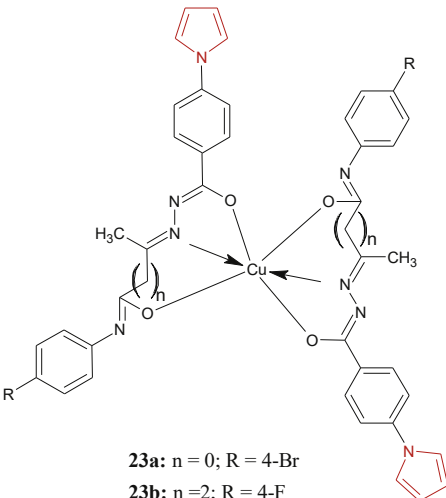
3. Antimicrobial activity

Nowadays, resistance to antimicrobial drugs is one of the major problems strongly afflicting human health and welfare. The huge use of antibacterials, both in human medicine and agriculture, has favored the development of bacterial resistance to different drugs, leading to multi-drug resistance and making gold standard treatments in bacterial chemotherapy ineffective [46]. Table 3 shows the main antimicrobial targets addressed by pyrrole-based compounds.

3.1. Sortase A (SrtA) inhibitors

Sortase A is a transpeptidase responsible for covalently anchoring many surface proteins in Gram-positive peptidoglycan, thus encouraging adhesion and biofilm formation. The inhibition of SrtA is related to the attenuation of virulence in *Staphylococcus aureus* and also in other important Gram-positive pathogens as *Listeria monocytogenes*, *Streptococcus pneumoniae*, and *Streptococcus mutans* [47–50]. With the aim to investigate the mechanism of action of pyrrolomycins [51–55,57,58], in 2019, Raimondi et al. [59] prepared six pyrrolomycins *via* microwave-assisted synthesis. All compounds exhibited good inhibitory activity towards SrtA with IC₅₀ values (130–300 μM) comparable to berberine hydrochloride (120 μM). The best pyrrolomycin was **22** both in inhibiting biofilm formation of *S. aureus* ATCC 25923 and in the SrtA enzyme assay, showing a lower IC₅₀ value (140 μM) than reference compound **F_{2a}** (250 μM). Docking studies revealed the interactions of the pyrrolomycins within the SrtA active site (PDB ID: 1T2W), as showed in Fig. 2. The inhibitory activity on biofilm formation was affected by

Table 3
Antimicrobial activity of pyrrole derivatives **22–23**.

Targets	Chemical structures
SrtA	 <p>22: R¹ = R² = R³ = R⁴ = R⁵ = Br F_{2a}: R¹ = R³ = R⁴ = Br; R² = Cl; R⁵ = H</p>
ENR	 <p>23a: n = 0; R = 4-Br 23b: n = 2; R = 4-F</p>

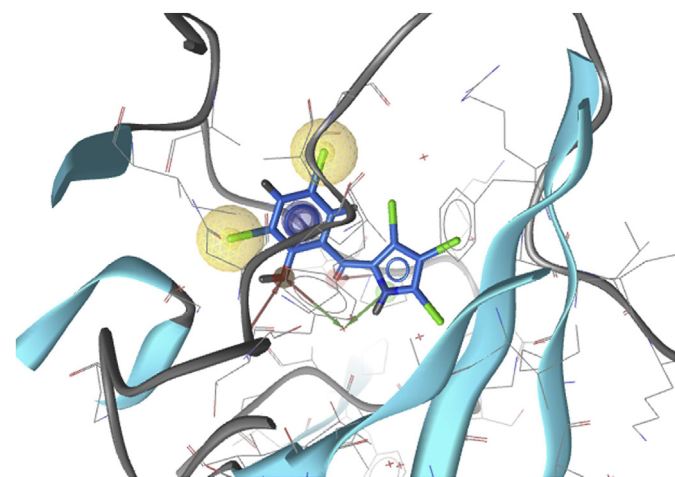


Fig. 2. Observed binding mode of compound **22** (blue stick) docked into the crystal structure of Sortase A (PDB ID: 1T2W) and examined by LigandScout® version 4.4 Expert (Inte:Ligand, GmbH). Green and red arrows represent donor and acceptor hydrogen bonds, respectively; yellow spheres represent hydrophobic interactions; blue disk represents interactions with an aromatic ring. (For interpretation of the references to color in this figure legend, the reader is referred to the Web version of this article.)

the degree of halogenation. In fact, while **F_{2a}**, characterized by tetra-halogen substituents, inhibited biofilm formation of *S. aureus* with an IC₅₀ value of 7.8 nM, pentabromide **22** exhibited a higher biofilm inhibitory activity with IC₅₀ = 3.4 nM.

3.1.1. 2-Trans-enoyl-acyl carrier protein reductase (InhA) inhibitors

The enoyl-ACP reductase of the fatty acid synthase-II (FAS-II) system is involved in the biosynthesis of mycolic acids, a major constituent of mycobacterial cell walls. It catalyzes the NADH-dependent reduction of the double bond of 2-*trans*-enoyl-acyl-carrier protein, a crucial step in the fatty acid elongation cycle of the FAS-II pathway. In 2016, Joshi et al. [60] synthesized a series of pyrrolyl hydrazones and their copper complexes to test the *in vitro* antitubercular activity of these compounds against *Mycobacterium tuberculosis*. The metal complexes **23a,b** exhibited the highest antitubercular activity with MICs of 0.8 µg/mL, being slightly higher than the MIC of the reference drug rifampicin (0.4 µg/mL). An *in vitro* enzyme inhibition assay against InhA from *M. tuberculosis* showed that complex **23b** and the respective metal-free ligand caused (nearly) 100% inhibition of the enzyme at 50 µM and exhibited a similar activity profile against InhA (IC₅₀s of 2.4 and 7.7 µM for **23b** and its ligand, respectively). Whereas the ligand of copper complex **23a** caused 35% inhibition, complex **23a** completely inhibited InhA activity at 50 µM, displaying an IC₅₀ value of 2.4 µM. Docking studies on the isoniazid resistant I47T enoyl-ACP reductase (ENR) mutant enzyme from *M. tuberculosis* (PDB ID: 2AQJ) confirmed the interactions between the complexes and the mutant ENR enzyme. Taken together, these results evidenced that *p*-halogens on the anilide ring were favourable for biological activity, both the anti-TB activity and the binding interaction with the mutant ENR enzyme, with the complexes showing lower MICs than the metal-free ligands.

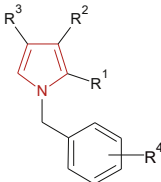
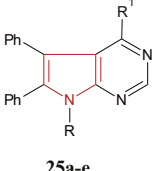
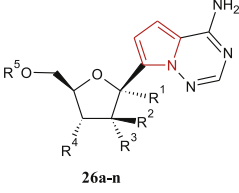
4. Antiviral agents

Viruses are the smallest organisms belonging to the largest group of pathogens able to infect animals, plants, and bacterial cells, which they use to replicate. As a consequence, they are responsible for several pathological conditions. Based on their targets, antiviral agents are divided into two groups, namely (i) inhibitors that target the viruses themselves or (ii) inhibitors that target host cell factors [61]. Nevertheless, many antiviral pharmaceuticals fail in the clinic mainly due to the emergence of recombinant viruses, drug resistance and cell toxicity [62,63]. Table 4 shows the main antiviral targets of pyrrole-based compounds.

4.1. HIV-1 integrase (IN) inhibitors

The integrase (IN) is a key enzyme involved in the HIV-1 replication cycle and is responsible for the chromosomal incorporation of the newly synthesized double-stranded viral DNA copy into the host genomic DNA. IN is involved in a large nucleoprotein assembly, called the pre-integration complex, which exerts 3'-processing and strand transfer reactions. Both activities require enzyme multimerization and coordination of the nucleic acid substrate by two Mg²⁺ ions within the IN catalytic core. In 2016, Corona and co-workers [64] have investigated the ability of pyrrolyl-diketoacids (DKA) to inhibit HIV-1 replication by interacting with the Mg²⁺ cofactors within the HIV-1 IN active site and within the HIV-1 reverse-transcriptase associated RNase H active site. The study was carried out by investigating the binding mode of four pyrrolyl-DKA (**24a-d**) in the HIV-1 IN active site (PDB ID: 3OYA) coupled with site-directed mutagenesis studies (Fig. 3), experimentally showing that the pyrrolyl-DKA scaffold interacts mainly with the IN amino acid residues Pro145, Gln146, and Gln148. Notably, the diketoacids revealed a good efficacy against HIV-1 raltegravir resistant Y143A and N155H INs. The insertion of diketoacids at positions 2 and 3 of the pyrrole ring led to selective anti-INs (**24a-d**), whereas a dual anti-IN/RNase H profile was shown by

Table 4
Antiviral pyrrole derivatives 24–26.

Targets	Chemical structures
HIV-1 Integrase (IN)	 <p>24a-d</p> <p>24a: R¹ = H; R² = C(O)CHC(OH)COOH; R³ = C₆H₅; R⁴ = 4-F 24b: R¹ = CHCHC(O)CHC(OH)COOH; R² = H; R³ = H; R⁴ = 4-F 24c: R¹ = H; R² = CHCHC(O)CHC(OH)COOH; R³ = C₆H₅; R⁴ = 4-F 24d: R¹ = CHCHC(O)CHC(OH)COOH; R² = H; R³ = H; R⁴ = 3-OCH₃</p>
Non-structural protein 5B (NS5B)	 <p>25a-e</p> <p>25a: R = 4-Cl-C₆H₄; R¹ = NH(2-CH₃)C₆H₄ 25b: R = 3-Cl-C₆H₄; R¹ = NH(2-CH₃)C₆H₄ 25c: R = C₆H₁₁; R¹ = Cl 25d: R = 4-Cl-C₆H₄; R¹ = NHNC(4-Cl)C₆H₄ 25e: R = 3-Cl-C₆H₄; R¹ = NHNC(4-Cl)C₆H₄</p>
RNA dependent RNA polymerase (RdRp)	 <p>26a-n</p> <p>26a (Sp isomer): R¹ = CN; R² = H; R³ = R⁴ = OH; R⁵ = phosphoramidate 26b (Sp and Rp, 1:1 isomers): R¹ = CN; R² = H; R³ = R⁴ = OH; R⁵ = phosphoramidate 26c (Rp isomer): R¹ = CN; R² = H; R³ = R⁴ = OH; R⁵ = phosphoramidate 26d: R¹ = CN; R² = R³ = H; R⁴ = OH 26e: R¹ = R² = R³ = H; R⁴ = OH 26f: R¹ = CH₃; R² = R³ = H; R⁴ = OH 26g: R¹ = CCH; R² = R³ = H; R⁴ = OH 26h: R¹ = CCH; R² = H; R³ = R⁴ = OH; R⁵ = phosphoramidate 26i: R¹ = CN; R² = R³ = H; R⁴ = F; R⁵ = OH 26j: R¹ = CN; R² = CH₃; R³ = R⁴ = OH; R⁵ = H 26k: R¹ = CN; R² = CH₃; R³ = R⁴ = OH; R⁵ = phosphoramidate 26l: R¹ = CN; R² = CH₃; R³ = OH; R⁴ = OC(O)CH(CH₃)₂; R⁵ = phosphoramidate 26m: R¹ = CN; R² = H; R³ = R⁴ = OH; R⁵ = triphosphate 26n: R¹ = CN; R² = CH₃; R³ = R⁴ = OH; R⁵ = triphosphate</p> <p>Phosphoramidate</p>

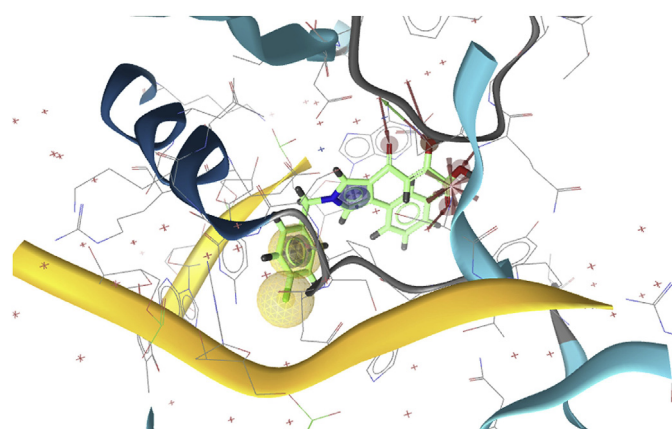


Fig. 3. Observed binding mode of compound **24a** (green stick) docked into the Prototypic Foamy Virus (PFV) intasome (PDB ID: 3OYA) and examined by LigandScout® version 4.4 Expert (Inte:Ligand, GmbH). Green and red arrows represent donor and acceptor hydrogen bonds, respectively; yellow spheres represent hydrophobic interactions; blue disks represent interactions with aromatic rings; red aura represents a negative ionizable area. (For interpretation of the references to color in this figure legend, the reader is referred to the Web version of this article.)

diketoesters. Additionally, the presence of a *p*-fluoro-benzyl substituent and an additional phenyl ring inserted at position 4 of the pyrrole ring seemed to be crucial to obtain a dual IN/RNase H inhibitor.

4.2. Non-nucleoside HCV non-structural protein 5B (NS5B) polymerase inhibitors

The non-structural protein 5B (NS5B) is a RNA-dependent RNA polymerase crucial for the replication of the hepatitis C virus. Its role consists in the polymerization of ribonucleoside triphosphates using RNA as a template for *de novo* synthesis. Mohamed and collaborators [65] synthesized a series of pyrrolo[2,3-d]pyrimidines and pyrrolo[3,2-e] [1,2,4]triazolo[4,3-c]pyrimidines with antiviral activity against HCV. Five derivatives (**25a-e**) out of fifty-seven compounds showed considerable antiviral activity, causing a reduction of the virus titer of 90, 76.7, 73.3, 70, and 63.3%, respectively, associated with low toxicity. SAR investigations indicated that the 5,6-diphenyl-7-(3- or 4-chlorophenyl)pyrrolo[2,3-d]pyrimidines, suitably substituted at position 4 with a chlorine or an arylamino group (**25a-c**), could be a useful scaffold for anti-HCV agents. The binding mode was predicted by docking studies (PDB ID: 3GOL), through which the interactions between the HCV NS5B polymerase enzyme and the new derivatives were established.

4.3. RNA-dependent RNA polymerase (RdRp) inhibitors for Ebola virus disease

The Ebola virus (EBOV) is a negative-sense single-stranded RNA virus responsible for an acute infection characterized by haemorrhagic fever. Viral replication on macrophages and dendritic cells induces the production of proinflammatory cytokines, chemokines,

and tissue factor, triggering vasodilation, increased vascular permeability, and diffuse intravascular coagulation. In 2016, Warren et al. [66] published the biological results of the pyrrolo[2,1-*f*]triazin-4-amino derivative **26a**, a phosphoramidate prodrug of an adenosine analogue, being suitable for the treatment of EBOV and other human RNA viruses. The mechanism of action identified in human monocyte-derived macrophages comprises the formation of the respective nucleoside triphosphate (NTP). Acting as an alternative substrate, the NTP inhibits the RdRp-catalysed RNA synthesis by being incorporated into the nascent viral RNA transcript, thus triggering its premature termination. Compound **26a** was active against a broad range of *filoviruses* including EBOV with EC₅₀s of 0.06–0.14 μM. An *in vivo* efficacy study in EBOV-infected rhesus monkeys showed a reduction in systemic viremia and improved survival by 33%. The interesting results prompted the authors [67] to screen a library of about a thousand nucleoside and nucleoside phosphonate analogs of **26a** and test their activity against a panel of RNA viruses, such as EBOV, respiratory syncytial virus (RSV), and HCV-1b. Their toxicity profile was evaluated in MT4 (human T cell leukemia), HEp-2 (human epithelial type 2), and Huh-7 (human liver) cell lines.

Among the synthesized compounds, **26a** proved to be still the best analog on the RNA virus panel, with submicromolar EC₅₀s of 0.015–0.10 μM and a good toxicity profile (CC₅₀ = 1.7–36 μM). Similar results were also obtained with the mixture of diastereomers **26b** (Sp and Rp isomers ~1:1), which showed anti-viral activity with EC₅₀s of 0.023–0.17 μM and a toxicity profile of 2–17 μM.

Starting from compound **26d**, which lacks the phosphoramidate moiety, SAR was investigated. The presence of the 1'-CN group of **26d** was fundamental for the selectivity towards viral RdRp and avoiding toxicity, as demonstrated by the unmodified C-nucleoside **26e**, which showed poor selectivity (CC₅₀ = 0.01–0.15 μM). The 1'-methyl derivative **26f** was less active against EBOV and also showed a higher degree of toxicity than **26d**, displaying how small modifications in the polarity and size of the 1'-substituent can affect the overall profile. The 1'-ethynyl analog **26g** and its corresponding 2-ethylbutyl phosphoramidate prodrug **26h** were both less active than their 1'-CN analogs (**26d** and **26b**, respectively). The 2'-deoxy-2'-fluorine (**26i**) and 2'-β-methyl (**26j**) analogs both lacked antiviral activity, while the 2'-β-methyl phosphoramidate prodrugs **26k,l** were both potent against HCV with EC₅₀s of 0.37 and 0.31 μM, respectively. Finally, the role of the *N*-heterocycle was investigated. The replacement of the pyrrolo[2,1-*f*]triazin-4-amino (**26d**) by a purin-6-amino moiety resulted in a decrease in activity against all viruses (EC₅₀s of 44–100 μM), while the replacement by a 4-aminopyrimidin-2-one core provided weak antiviral activity only against RSV and HCV-1b (EC₅₀ = 7.3 and 12 μM, respectively). However, the activity profile on HCV-1b of the 4-aminopyrimidin-2-one derivative could be slightly improved by the introduction of a phosphoramidate moiety (EC₅₀ = 2.5 μM).

To confirm that the anti-viral activities were due to the formation of an NTP moiety, the metabolite **26m** was tested on viral RdRps. The triphosphate **26m** showed interesting inhibitory activities on RSV-RdRp and HCV-RdRp with IC₅₀s of 1.1 and 5.0 μM, respectively. The inhibitory activity on EBOV-RdRp was obtained by measuring NTP levels inside the cells after 72 h of incubation with **26m** at 1 μM. C_{max} levels of 300, 110, and 90 pmol/million cells were achieved for **26m** in macrophages, HMVEC, and HeLa cell lines, respectively, supporting the potent antiviral efficacy of **26a**.

Computational studies with active NPT metabolites **26m** and **26n** in the crystal structures of HIV and HCV polymerases (PDB ID: 1RTD and 4WTG) were performed, confirming the importance of the 1'-CN group, which occupies a binding pocket presents in both polymerases. The docking results were useful for prodrug

optimization and led the authors to synthesize thirteen analogs of **26a** bearing different amino acid esters. The biological results indicated that the increased steric hindrance generally produces compounds being less active than **26a**. In fact, all new compounds showed lower EBOV inhibitory activity in all cell lines (EC₅₀s of 0.088–30.41 μM) compared to **26a** (EC₅₀s of 0.053–0.100 μM).

5. Concluding remarks

Among heterocycles, pyrrole and its hetero-fused derivatives are widely presented in many natural compounds with a broad spectrum of biological activities. Therefore, for several years, these *N*-heterocycles have attracted much attention among medicinal chemists as valuable scaffolds to achieve synthetic analogs with pharmacological activity, some of which are of clinical interest. This review is focused on the pyrrole scaffold as the main structural feature of novel bioactive compounds within selected therapeutic areas, such as anticancer, antimicrobial, and antiviral, reported in the literature between 2015 and 2019. The promising biological results collected in this review underline the importance of the pyrrole core in bioactive molecules and will help the scientific community to identify new and powerful derivatives based on the pyrrole framework.

Funding source

No funds were used to carry out this research.

Declaration of competing interest

The authors declare that they have no known competing financial interests or personal relationships that could have appeared to influence the work reported in this paper.

Abbreviations

A375	human melanoma
A549	lung carcinoma
ALK	anaplastic lymphoma kinase
AURKA	aurora kinase A
BaP	benzo[a]pyrene
CA-4	combretastatin A-4
CAMK1	calcium/calmodulin-dependent protein kinase type 1
CC ₅₀	50% cytotoxic concentration
CEMV ^{bl100}	acute T lymphoblastic leukemia
CSF-1	colony stimulating factor 1
CYP	cytochrome-P450
EBOV	Ebola virus
EC ₅₀	half maximal effective concentration
EGFR	epidermal growth factor receptor
EML4	echinoderm microtubule associated protein like 4
EMSA	electrophoretic mobility shift assay
enoyl-ACP	enoyl-acyl carrier protein
ENR	enoyl-ACP reductase
Eph	ephrin
ERK1	extracellular signal-regulated kinase 1
FAS-II	fatty acid synthase-II
FDA	food and drug administration
FGFR4	fibroblast growth factor receptor 4
FMS	Feline McDonough Sarcoma
GI ₅₀	cells growth inhibition of 50%
HCT116	colon cancer
HCV	Human Hepatitis C virus
HEK293	human embryonic kidney epithelial
HeLa	cervix epithelial adenocarcinoma

HEp-2	human epithelial type 2
HFF-1	normal fibroblast
HGF/SF	hepatocyte growth factor/scatter factor
HIF-1 α /-2 α /-3 α	hypoxia-inducible factor-1 α /-2 α /-3 α
HIV	human immunodeficiency virus
HL-60	acute promyelocytic leukemia
HT-29	colorectal adenocarcinoma
Huh-7	human liver
IC ₅₀	half maximal inhibitory concentration
ICB2	inverted CCAAT box 2
IN	integrase
JNK2	c-Jun N-terminal kinase isoform 2
MAPKAP-K3	MAP kinase-activated protein kinase 3
MCF-7	breast cancer
M-CSF	macrophage colony-stimulating factor
MDA-MB-231	triple-negative breast cancer
MIC	minimum inhibitory concentration
MINK1	misshapen-like kinase 1
MT4	human T cell leukemia
MTs	microtubules
NF-Y	Nuclear Factor-Y;
NPM	nucleophosmin
NTP	nucleoside triphosphate
PARP	poly(ADP-ribose)polymerase
PC-3	prostatic cancer
PDB ID	protein data bank identification code
PDGFR	platelet-derived growth factor receptor
PKCa	protein kinase C alpha
PIGF	placental growth factor
pyrrolyl-DKA	pyrrolyl-diketoacids
RdRp	RNA-dependent RNA polymerase
ROS	reactive oxygen species
RTK	receptor tyrosine kinase
SAR	structure-activity relationships
SKBR3	breast cancer
Tie2	angiopoietin receptor
TIM	transforming immortalized mammary
topo-II α	topoisomerase-II α
TrkA	tropomyosin receptor kinase A
VEGF-A/B/C/D	vascular endothelial growth factor-A/B/C/D
VEGFR-1/2/3	vascular endothelial growth factor receptor-1/2/3

Appendix A. Supplementary data

Supplementary data to this article can be found online at <https://doi.org/10.1016/j.ejmech.2020.112783>.

References

- [1] N.E. Thomford, D.A. Senthane, A. Rowe, D. Munro, P. Seele, A. Maroyi, K. Dzobo, Natural products for drug discovery in the 21st Century: Innovations for novel drug discovery, *Int. J. Mol. Sci.* 19 (2018), <https://doi.org/10.3390/ijms19061578>.
- [2] A. Gomtsyan, Heterocycles in drugs and drug discovery, *Chem. Heterocycl. Compd.* 48 (2012) 7–10, <https://doi.org/10.1007/s10593-012-0960-z>.
- [3] X.H. Ma, Z. Shi, C. Tan, Y. Jiang, M.L. Go, B.C. Low, Y.Z. Chen, In-silico approaches to multi-target drug discovery, *Pharm Res* 27 (2010) 739–749, <https://doi.org/10.1007/s11095-010-0065-2>.
- [4] B. Maggio, D. Raffa, M.V. Raimondi, F. Plescia, M.L. Trincavelli, C. Martini, F. Meneghetti, L. Basile, S. Guccione, G. Daidone, Synthesis, benzodiazepine receptor binding and molecular modelling of isochromeno[4,3-c]pyrazol-5(1H)-one derivatives, *Eur. J. Med. Chem.* 54 (2012) 709–720, <https://doi.org/10.1016/j.ejmech.2012.06.028>.
- [5] A. Lauria, C. Patella, P. Diana, P. Barraja, A. Montalbano, G. Cirrincione, G. Dattolo, A.M. Almerico, A synthetic approach to new polycyclic ring system of biological interest through domino reaction: indolo[2,3-e][1,2,3]triazolo [1,5-a]pyrimidine, *Tetrahedron Lett.* 47 (2006) 2187–2190, <https://doi.org/10.1016/j.tetlet.2006.01.112>.
- [6] D. Raffa, B. Maggio, F. Plescia, S. Cascioferro, M.V. Raimondi, G. Cancemi, A. D'Anneo, M. Lauricella, M.G. Cusimano, R. Bai, E. Hamel, G. Daidone, Synthesis, antiproliferative activity and possible mechanism of action of novel 2-acetamidobenzamides bearing the 2-phenoxy functionality, *Bioorg. Med. Chem.* 23 (2015) 6305–6316, <https://doi.org/10.1016/j.bmc.2015.08.027>.
- [7] S. Alcaro, F. Ortuso, Multi-target drug discovery: an opportunity for novel and repurposed bioactive compounds, *Eur. J. Med. Chem.* 192 (2020) 112188, <https://doi.org/10.1016/j.ejmech.2020.112188>.
- [8] G. Costa, R. Rocca, A. Corona, N. Grandi, F. Moraca, I. Romeo, C. Talarico, M.G. Gagliardi, F.A. Ambrosio, F. Ortuso, S. Alcaro, S. Distinto, E. Maccioni, E. Tramontano, A. Artese, Novel natural non-nucleoside inhibitors of HIV-1 reverse transcriptase identified by shape- and structure-based virtual screening techniques, *Eur. J. Med. Chem.* 161 (2019) 1–10, <https://doi.org/10.1016/j.ejmech.2018.10.029>.
- [9] G.A. Patani, E.J. LaVoie, Bioisosterism: A rational approach in drug design, *Chem. Rev.* 96 (1996) 3147–3176, <https://doi.org/10.1021/cr950066q>.
- [10] B. Maggio, M.V. Raimondi, D. Raffa, F. Plescia, S. Cascioferro, G. Cancemi, M. Tolomeo, S. Grimaudo, G. Daidone, Synthesis and antiproliferative activity of 3-(2-chloroethyl)-5-methyl-6-phenyl-8-(trifluoromethyl)-5,6-dihydropyrazolo[3,4-f][1,2,3,5]tetrazepin-4-(3H)-one, *Eur. J. Med. Chem.* 96 (2015) 98–104, <https://doi.org/10.1016/j.ejmech.2015.04.004>.
- [11] G. Daidone, A. D'Anneo, M.V. Raimondi, D. Raffa, E. Hamel, F. Plescia, M. Lauricella, B. Maggio, New complex polycyclic compounds: synthesis, antiproliferative activity and mechanism of action, *Bioorg. Chem.* 101 (2020) 103989, <https://doi.org/10.1016/j.bioorg.2020.103989>.
- [12] E. Vitaku, D.T. Smith, J.T. Njardarson, Analysis of the structural diversity, substitution patterns, and frequency of nitrogen heterocycles among U.S. FDA approved pharmaceuticals, *J. Med. Chem.* 57 (2014) 10257–10274, <https://doi.org/10.1021/jm501100b>.
- [13] P. Martins, J. Jesus, S. Santos, L.R. Raposo, C. Roma-Rodrigues, P.V. Baptista, A.R. Fernandes, Heterocyclic anticancer compounds: recent advances and the paradigm shift towards the use of nanomedicine's tool box, *Molecules* 20 (2015) 16852–16891, <https://doi.org/10.3390/molecules200916852>.
- [14] K.W. Chan, V.T. Wong, S.C.W. Tang, COVID-19: an update on the epidemiological, clinical, preventive and therapeutic evidence and guidelines of integrative Chinese-western medicine for the management of 2019 novel coronavirus disease, *Am. J. Chin. Med.* (2020) 1–26, <https://doi.org/10.1142/S0192415X20500378>.
- [15] C. Wu, Y. Liu, Y. Yang, P. Zhang, W. Zhong, Y. Wang, Q. Wang, Y. Xu, M. Li, X. Li, M. Zheng, L. Chen, H. Li, Analysis of therapeutic targets for SARS-CoV-2 and discovery of potential drugs by computational methods, *Acta Pharmaceutica Sinica B* 10 (5) (2020) 766–788, <https://doi.org/10.1016/j.apsb.2020.02.008>.
- [16] R.L. Siegel, K.D. Miller, A. Jemal, Cancer statistics, *CA A Cancer J. Clin.* 70 (2020) 7–30, <https://doi.org/10.3322/caac.21590>, 2020.
- [17] R.L. Siegel, K.D. Miller, A. Jemal, Cancer statistics, *CA A Cancer J. Clin.* 69 (2019) 7–34, <https://doi.org/10.3322/caac.21551>, 2019.
- [18] Y.T. Lee, Y.J. Tan, C.E. Oon, Molecular targeted therapy: Treating cancer with specificity, *Eur. J. Pharmacol.* 834 (2018) 188–196, <https://doi.org/10.1016/j.ejphar.2018.07.034>.
- [19] M.V. Raimondi, O. Randazzo, M. La Franca, G. Barone, E. Vignoni, D. Rossi, S. Collina, DHFR inhibitors: Reading the past for discovering novel anticancer agents, *Molecules* 24 (2019) 1140, <https://doi.org/10.3390/molecules24061140>.
- [20] D.M. Corigliano, R. Syed, S. Messineo, A. Lupia, R. Patel, C.V.R. Reddy, P.K. Dubey, C. Colica, R. Amato, G. De Sarro, S. Alcaro, A. Indrasena, A. Brunetti, Indole and 2,4-Thiazolidinedione conjugates as potential anticancer modulators, *PeerJ* 6 (2018) e5386, <https://doi.org/10.7717/peerj.5386>.
- [21] S. Raychaudhuri, A minimal model of signaling network elucidates cell-to-cell stochastic variability in apoptosis, *PLoS One* 5 (2010), e11930, <https://doi.org/10.1371/journal.pone.0011930>.
- [22] Z. Kilic-Kurt, F. Bakar-Ates, Y. Aka, O. Kutuk, Design, synthesis and in vitro apoptotic mechanism of novel pyrrolopyrimidine derivatives, *Bioorg. Chem.* 83 (2019) 511–519, <https://doi.org/10.1016/j.bioorg.2018.10.060>.
- [23] T. Mitchison, M. Kirschner, Dynamic instability of microtubule growth, *Nature* 312 (1984) 237–242, <https://doi.org/10.1038/312237a0>.
- [24] D. Carta, R. Bortolozzi, M. Sturlese, V. Salmaso, E. Hamel, G. Basso, L. Calderan, L. Quintieri, S. Moro, G. Viola, M.G. Ferlin, Synthesis, structure-activity relationships and biological evaluation of 7-phenyl-pyrroloquinolinone 3-amide derivatives as potent antimetabolic agents, *Eur. J. Med. Chem.* 127 (2017) 643–660, <https://doi.org/10.1016/j.ejmech.2016.10.026>.
- [25] R. Bortolozzi, E. Mattiuzzo, M. Dal Pra, M. Sturlese, S. Moro, E. Hamel, D. Carta, G. Viola, M.G. Ferlin, Targeting tubulin polymerization by novel 7-aryl-pyrroloquinolinones: synthesis, biological activity and SARs, *Eur. J. Med. Chem.* 143 (2018) 244–258, <https://doi.org/10.1016/j.ejmech.2017.11.038>.
- [26] R. Bortolozzi, D. Carta, M.D. Prà, G. Antoniazzi, E. Mattiuzzo, M. Sturlese, V. Di Paolo, L. Calderan, S. Moro, E. Hamel, L. Quintieri, R. Ronca, G. Viola, M.G. Ferlin, Evaluating the effects of fluorine on biological properties and metabolic stability of some antitubulin 3-substituted 7-phenyl-pyrroloquinolinones, *Eur. J. Med. Chem.* 178 (2019) 297–314, <https://doi.org/10.1016/j.ejmech.2019.05.092>.
- [27] M. Brindisi, C. Ulivieri, G. Alfano, S. Gemma, F. de Asis Balaguer, T. Khan, A. Grillo, G. Chemi, G. Menchon, A.E. Prota, N. Olieric, D. Lucena-Agell, I. Barasoain, J.F. Diaz, A. Nebbioso, M. Conte, L. Lopresti, S. Magnano, R. Amet, P. Kinsella, D.M. Zisterer, O. Ibrahim, J. O'Sullivan, L. Morbidelli, R. Spaccapelo, C. Baldari, S. Butini, E. Novellino, G. Campiani, L. Altucci, M.O. Steinmetz, S. Bardi, Structure-activity relationships, biological evaluation and structural studies of novel pyrrolonaphthoxazepines as antitumor agents, *Eur. J. Med.*

A.L. Rheingold, A.S. Ray, R. Bannister, R. Strickley, S. Swaminathan, W.A. Lee, S. Bavari, T. Cihlar, M.K. Lo, T.K. Warren, R.L. Mackman, Discovery and synthesis of a phosphoramidate prodrug of a pyrrolo[2,1-f][triazin-4-amino]

adenine C-nucleoside (GS-5734) for the treatment of Ebola and emerging viruses, *J. Med. Chem.* 60 (2017) 1648–1661, <https://doi.org/10.1021/acs.jmedchem.6b01594>.